Articles

Structural Characterization of Yeast Acidic Ribosomal P Proteins Forming the P1A−P2B Heterocomplex†

Marek Tchórzewski,*,‡ Dawid Krokowski,‡ Aleksandra Boguszewska,‡ Anders Liljas,§ and Nikodem Grankowski‡

Institute of Microbiology and Biotechnology, Department of Molecular Biology, Maria Curie-Skłodowska University, Akademicka Street 19, 20-033 Lublin, Poland, and Center for Chemistry and Chemical Engineering, Department of Molecular Biophysics, Lund University, Box 124, 221 00 Lund, Sweden

Received September 26, 2002; Revised Manuscript Received December 13, 2002

ABSTRACT: Acidic ribosomal P proteins form a distinct lateral protuberance on the 60S ribosomal subunit. In yeast, this structure is composed of two heterocomplexes (P1A−P2B and P1B−P2A) attached to the ribosome with the aid of the P0 protein. In solution, the isolated P proteins P1A and P2B have a flexible structure with some characteristics of a molten globule [Zurdo, J., et al. (2000) *Biochemistry 39*, 8935−8943]. In this report, the structure of P1A−P2B heterocomplex from *Saccharomyces cerevisiae* is investigated by means of size-exclusion chromatography, chemical cross-linking, circular dichroism, light scattering, and fluorescence spectroscopy. The circular dichroism experiment shows that the complex could be ranked in the tertiary class of all-α proteins, with an average α-helical content of ∼65%. Heat and urea denaturation experiments reveal that the P1A−P2B complex, unlike the isolated proteins, has a full cooperative transition which can be fitted into a two-state folding−unfolding model. The behavior of the complex in the presence of 2,2,2-trifluoroethanol also resembles a two-state folding−unfolding transition, further supporting the idea that the heterocomplex contains well-packed side chains. In conclusion, the P1A−P2B heterocomplex, unlike the isolated proteins, has a well-defined hydrophobic core. Consequently, the complex can put up its structure without additional ribosomal components, so the heterodimeric complex reflects the intrinsic properties of the two analyzed proteins, indicating thus that this is the only possible configuration of the P1A and P2B proteins on the ribosomal stalk structure.

Proteins are normally cooperatively folded into a compact and specific conformation. They are optimized and highly specialized for a specific biological task via precise three-dimensional arrangements of functional groups. Although the function of many proteins is directly related to their three-dimensional structure, numerous proteins that lack an intrinsic globular structure under physiological conditions have nowadays been recognized. Disorder in proteins can be either local or global. Locally disordered regions are common and have been observed in numerous X-ray and NMR structure of proteins; in some cases, such disordered regions have been linked to biological function. So far, well-characterized examples of global disorder have been rare (*1*). For example, such intrinsically unfolded proteins have been found among ribosomal proteins, with a prominent example being the yeast P1A and P2B proteins. It has been suggested that these proteins have a so-called molten globule-like structure in solution (*2*, *3*). Such a state is usually characterized by partial retention of the secondary structure of the native state, but with the loss of the tertiary structure, giving rise to a compact structure without rigid packing inside the molecule (*4*).

P1A and P2B proteins belong to the family of acidic ribosomal P proteins, forming a lateral protuberance (called a stalk structure) on the 60S ribosomal subunit (*5*). This structure is thought to be responsible for interactions with translation factors during the course of protein synthesis. In eukaryotes, the P proteins are categorized into two groups, P1 and P2 (*6*), with the exception of plants, which contain an extra P3 group (*7*). Lower-eukaryotic cells, such as the yeast *Saccharomyces cerevisiae*, have two forms of P1 and P2, P1A−P1B and P2B−P2A, respectively (*8*). Recently, it has been found that yeast or mammalian P proteins are able to form the P1−P2 heterocomplex structure (*9*−*12*) which is attached to the ribosomal structure through the P0 protein, where the P1 protein plays an essential role as an anchor of the heterocomplex (*13*, *14*). The domain responsible for heterodimer formation and for interaction with the P0 proteins is the N-terminal part of the polypeptide, while the C-terminal fragment has a flexible hinge and an intriguing 11-amino acid sequence, extremely well preserved in all

† This work was supported by State Committee for Scientific Research (KBN) Grant 6P04A 050 21, and partially by the Royal Swedish Academy of Science as a Swedish-Polish joint research project.

* To whom correspondence should be addressed: Institute of Microbiology and Biotechnology, Department of Molecular Biology, Maria Curie-Skłodowska University, Akademicka St. 19, 20-033 Lublin, Poland. Phone: +48 81 5375956. Fax: +48 81 5375907. E-mail: tchorz@biotop.umcs.lublin.pl.

‡ Maria Curie-Skłodowska University.

§ Lund University.

10.1021/bi0206006 CCC: $25.00
Published on Web 03/07/2003

eukaryotic organisms, from yeast to humans (*15*). The C-terminal part has a serine residue which is phosphorylated by several protein kinases (*16*). This modification has been implicated in several processes, such as protein−protein interactions (*10*, *17*), or may have a functional role related to P protein degradation, and might modulate the translation of specific proteins in response to some specific metabolic conditions (*18*, *19*). Yet the function of the eukaryotic stalk has not been fully revealed. As shown in yeast deletion mutants lacking the P1 and P2 proteins, the P proteins are not essential for ribosome activity; however, ribosomes depleted of P proteins selectively translate a different subset of mRNAs compared to "full ribosomes" (*20*). Additionally, the function of the transcriptional coactivator was attributed to P1 proteins from yeast (*21*). Furthermore, P proteins are able to interact with numerous proteins involved in DNA repair and transcription (*22*). The three-dimensional (3D) structure of the P proteins has not been determined so far; nevertheless, the tertiary structure of the stalk was recently observed using cryoelectron microscopy at 17.5 Å resolution (*23*). The stalk has an elongated structure only when forming a complex with elongation factor 2 and with sordarin which seems to immobilize this complex.

The prokaryotic stalk structure, equivalent to the eukaryotic one, is formed by the L12 protein (*24*). The prokaryotic protein is present in solution as a dimer. The structure of the L12 protein has been studied in great detail, showing that C- and N-terminal domains are well-defined compact structures joined by a "hinge" region (*25*, *26*). Several studies have shown that the hinge is unstructured and its flexibility is essential for protein activity (*27*, *28*); moreover, this is the only region to show some similarity to the hinge of eukaryotic P proteins, except that there is no significant similarity in the primary structure between two polypeptides from both kingdoms (*29*).

This report deals with a structural characterization of the yeast P1A−P2B heterocomplex, a counterpart of the prokaryotic L12 dimer. Since the L12 dimer has a folded structure in a solution, it was interesting to analyze the eukaryotic heterocomplex from a structural point of view. As described earlier, P1A and P2B *in vitro* alone lack a tertiary fold, but occur as a molten globule-like structure, and additionally, the analysis of the P1A and P2B mixture did not produce a decisive answer with regard to the nature of the heterocomplex, suggesting that interaction between both proteins might take place (*2*, *3*), the more so as the stalk structure was only seen on the ribosome in the complex with EF2 and sordarin (*23*). Thus, it appeared to be worth knowing when P1A and P2B proteins gain a stable tertiary structure: forming the P1A−P2B heterocomplex or after attaching them to the ribosomal structure. Different biophysical methods were used to obtain structural information. Experimental data indicate that upon forming the heterocomplex, both proteins are able to gain a compact though elongated structure under physiological conditions without additional ribosomal components. Therefore, this is the first thorough structural characterization of the ribosomal stalk constituents.

MATERIALS AND METHODS

Expression, Purification of Recombinant Proteins, and Heterocomplex Preparation. Recombinant proteins P1A and P2B were prepared according to the procedure established previously (*30*). The P1A−P2B heterocomplex was prepared by corenaturation of both recombinant proteins P1A and P2B as described recently (*10*). The complex was additionally purified by size-exclusion chromatography (SEC) using the ÄKTA Purifier FPLC system (Amersham Pharmacia Biotech) equipped with a Superose 12 HR 10/30 column.

Activity Test. 80S ribosomes were purified according to the procedure described earlier (*31*), from the *S. cerevisiae* W303-1b wild-type strain (α; *leu2-3,112, trp1-1, ura3-1, his3-11,15, ade2-1, can1-100*) or mutant strain D4567 (α; *RPY1*α*::LEU2, RPY1*β*::TRP1, RPYP2*α*::URA3, RPYP2*β*:: HIS3, can1-100*), which were derived from the wild-type W303-1b strain (*20*). For reconstitution of the stalk structure, ribosomes from the D4567 strain (0.75 nmol) were incubated with a 10-fold molar excess of the P1A−P2B heterocomplex in 20 mM Tris-HCl (pH 7.4), 12.5 mM $MgCl_2$, 80 mM KCl, and 5 mM β-mercaptoethanol (buffer A). Incubation was carried out for 12 h at 4 °C, and subsequently, the ribosomes were centrifuged through a 15% sucrose layer, then resuspended in buffer A, and used for an activity test or Western blotting. Polyphenylalanine synthesis was performed in a volume of 100 μL, containing 50 μg of 80S ribosomes, 90 μg of protein mixture prepared by ammonium sulfate precipitation (from 30 to 70%) of the S-100 fraction, 30 μg of [^{3}H]Phe-tRNA, 50 μg of poly(U), 1 mM GTP in 50 mM Tris-HCl (pH 7.4), 15 mM $MgCl_2$, 80 mM KCl, and 20 mM dithiothreitol. The reaction was carried out at 30 °C for 30 min, and then samples were precipitated with 10% trichloroacetic, boiled for 10 min, and finally filtered through the glass microfiber filters from Whatman International Ltd.

Light-Scattering Experiments. Light-scattering experiments were performed on DynaPro-801 (Protein Solutions, Charlottesville, VA) with a temperature-controlled microsampler at 20 °C, in 50 mM Tris-HCl (pH 7.5) and 150 mM NaCl. All data were analyzed with Dynamics version 5.24.02. Prior to measurements, special care was taken during the preparation of samples to avoid contamination with dust, as large dust particles might have dominated the scattering behavior. All solutions were passed through a 0.1 μm filter (Whatman International Ltd.) and then spun at 12000*g* for 45 min at 4 °C to force any remaining large dust particles to the bottom of the microcentrifuge tube. A 12 μL sample was used for each measurement, and the protein concentration was varied from 1 to 6 mg/mL. Values for the reported translational diffusion coefficiency D_T are statistical averages over at least 25 independent measurements. From the measured D_T, the hydrodynamic radius R_H was calculated using the Stokes−Einstein equation implemented in the software. The molecular mass was estimated from R_H using an empirically derived relationship between R_H and molecular mass for a number of well-characterized globular proteins.

Circular Dichroism Spectroscopy. Circular dichroism (CD) spectra were collected on a Jasco J-720 spectropolarimeter equipped with a PTC-343 peltier-type thermostatic cell holder, connected to a data station for signal averaging and processing. Far-UV CD spectra were usually acquired at 20 °C, and the protein concentration was 60 μg/mL, using PBS (phosphate-buffered saline) (pH 7.5) with the appropriate pH and 150 mM NaCl. For pH 2, glycine buffer was used [25 mM glycine (pH 2.1) and 150 mM NaCl]. The analysis was carried out in a cuvette with a 1 mm path. The obtained

spectra are averages of four scans and are reported as the mean residue ellipticity [Θ] (degrees per square centimeter per decimole), calculated from the equation

$$[\Theta] = (\Theta_{abs} \times 100M_r)/(cdN_A)$$

where Θ_{abs} is the measured ellipticity in degrees, c the protein concentration in milligrams per milliliter, d the path length in centimeters, M_r the molecular mass of the protein, and N_A the number of amino acids per protein. The factor of 100 originates from the conversion of the molar concentration to a concentration unit of decimoles per cubic centimeter.

CD temperature melting curves were determined by monitoring changes in the dichroic intensity at 222 nm as a function of temperature. For thermal denaturation experiments, in the range of 20−90 °C, a heating rate of 0.5 °C/min was applied using a peltier-type thermostatic cell holder. The protein concentration was 60 μg/mL. The reversibility of the thermal transition was checked after cooling the thermally denatured sample and subsequently recording a new scan under the same conditions.

Analysis of Equilibrium Unfolding. The urea-induced equilibrium unfolding transition curves for P1A−P2B heterocomplex, measured by CD spectroscopy, were analyzed assuming that this is a reversible two-state process from the folded dimer to the unfolded monomers (*32*, *33*):

$$N \underset{k_N}{\overset{k_U}{\leftrightarrow}} U$$

where N and U represent the native and reversible unfolded forms of the heterocomplex, respectively, and k_N and k_U the equilibrium constants of the unfolding transitions from the N to the U state and vice versa, respectively. The fraction of unfolded heterocomplex, f_U, is calculated from the relationship

$$f_N + f_U = 1$$

Denaturation changes at any denaturant concentration were determined by following ellipticity at 222 nm (Θ). The observed value of Θ at any point is given by the sum of the two states as

$$\Theta = \Theta_N f_N + \Theta_U f_U$$

where Θ_N and Θ_U represent values of Θ characteristic of the native and unfolded states, respectively. The f_N and f_U terms are related to the equilibrium, and k_N and k_U are related to the unfolding transitions from N to U and U and N, respectively, and hence related to the free energy of the unfolded form. Thus

$$f_U = (\Theta_F - \Theta)/(\Theta_F - \Theta_U)$$

The equilibrium constant, K, and free energy change of unfolding at any denaturant concentration, ΔG_U, can be calculated:

$$K = f_U/(1 - f_U) = f_U/f_F = (\Theta_F - \Theta)/(\Theta - \Theta_U)$$

and

$$\Delta G_U = -RT \ln K$$

where R is the gas constant (1.987 cal deg^{-1} mol^{-1}) and T is the absolute temperature. Values of Θ_F and Θ_U in the transition region were obtained by extrapolating from the pre- and post-transition regions.

To estimate the conformational stability in the absence of urea, ΔG^{H_2O}, we assumed a linear dependence of the free energy of unfolding on denaturant concentration to zero concentration. Hence, a least-squares analysis has been used to fit the data to this equation:

$$\Delta G_U = G_U^{H_2O} - m[\text{urea}]$$

where m is a measure of the dependence of ΔG on urea concentration. The denaturant concentration at the midpoint of the unfolding curve can be calculated:

$$[\text{UREA}]_{1/2} = \Delta G_U^{H_2O}/m$$

Size-Exclusion Chromatography (SEC). For our analyses, we used an Äkta Purifier FPLC system from Amersham Pharmacia Biotech, equipped with the Superose 12 HR 10/30 FPLC gel filtration column. The column was equilibrated with buffer [50 mM Tris-HCl (pH 7.8) and 150 mM NaCl]. Calibration of the column was carried out with a low-molecular mass protein standard provided by Amersham Pharmacia Biotech. The flow rate was 0.25 mL/min. The protein elution profile was monitored at 280 nm and analyzed using UNICORN version 4.0 which was included with the FPLC system.

Fluorescence Spectroscopy. Fluorescence spectra were recorded on a Perkin-Elmer luminescence spectrometer (LS50B) equipped with digital software. Samples of proteins were prepared at 0.2 μM in PBS (phosphate-buffered saline) (pH 7.5) or 20 mM Tris-HCl (pH 7.8) and 150 mM NaCl. Samples were excited at 280 or 295 nm, respectively. The intrinsic fluorescence emission spectra were collected in the 295−450 or 310−450 nm range, respectively, at a scan speed of 100 nm/min. Blank values without proteins were subtracted from the spectra.

Secondary Structure Analysis. Secondary structure prediction was made on the basis of amino acid sequences, using the EVA server (EValuation of Automatic protein structure prediction), a Web-based server that evaluates automatic structure prediction servers continuously and objectively (*34*). For prediction, the following programs were used: PSIpred (*35*), PHD (*36*), JPred (*37*), APSSP (*38*), PSSP (*38*), PROFsec (*39*), and SSPro2 (*40*). Estimation of the secondary structure content from far-UV circular dichroism (CD) spectra was performed using the CDPro software package. This software consists of three popular programs (SELCON3, CDSSTR, and CONTIN/LL), and an additional program for determination of the tertiary structure class (CLUSTER) (*41*, *42*). Furthermore, the K2D program (Kohonen neural network with a two-dimensional output layer) was also used for CD spectra analysis (*43*).

Miscellaneous. Chemical cross-linking of the recombinant ribosomal P proteins was performed as previously described (*10*). Protein concentrations were determined from the absorbance at 280 nm using an extinction coefficient (9530 M^{-1} cm^{-1}) calculated from the amino acid composition of the P1A−P2B heterocomplex according to the method described previously (*44*). SDS−PAGE was performed with

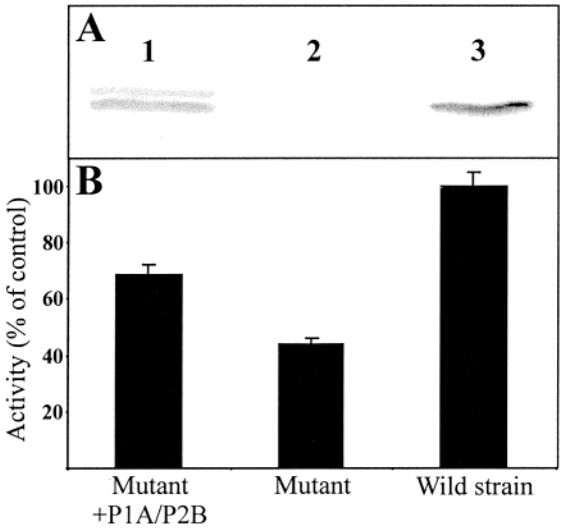

FIGURE 1: Translational activity analysis of *S. cerevisiae* ribosomes. (A) Western blotting of the ribosomal P proteins: lane 1, reconstituted ribosomes with the heterocomplex, where the upper protein band corresponds to the recombinant P1A protein having five additional amino acids; lane 2, ribosomes deprived of all P1 and P2 proteins; and lane 3, ribosomes from the wild-type strain. (B) Polymerizing activity of ribosomes. The activity of ribosomes from the *S. cerevisiae* W303-1b wild-type strain was taken as a control (100%): mutant + P1A/P2B, reconstituted ribosomes with the P1A−P2B heterocomplex; mutant, ribosomes deprived of all P1 and P2 proteins; and wild strain, ribosomes from wild-type strain W303-1b.

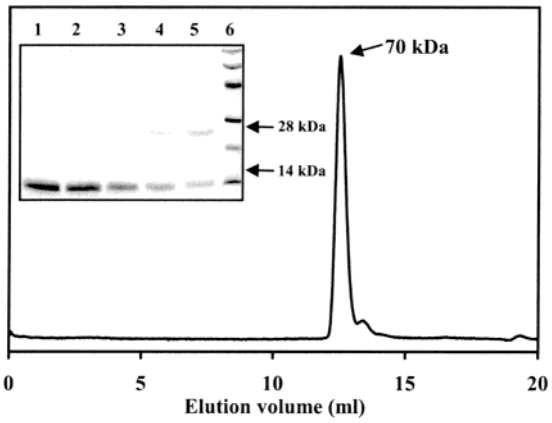

FIGURE 2: Analysis of the hetero-oligomeric complex of the P1A and P2B proteins by size-exclusion chromatography (SEC). The inset shows results of a cross-linking experiment of the hetero-complex P1A and P2B proteins after SEC analysis. Titration of the samples with time: lane 1, 0 min; lane 2, 5 min; lane 3, 10 min; lane 4, 15 min; lane 5, 30 min; and lane 6, protein markers, with molecular masses of 14, 20, 30, 45, 67, and 94 kDa.

the FAST system, according to the manufacturer's instructions (Amersham Pharmacia Biotech) or in a 14% acrylamide slab gel according to Laemmli's method (*45*). Western blotting was performed according to the previously described procedure with antibodies recognizing all yeast P proteins (*46*).

RESULTS

Ribosomal Activity Test

Polyphenylalanine Synthesis. Ribosomes from the quadruply disrupted strain, lacking all P1 and P2 proteins, were prepared and used for testing of the P1A−P2B heterocomplex toward its biological functionality. The P1A−P2B protein complex was able to bind to the ribosomal particles deprived of all P1 and P2 proteins (Figure 1A). Additionally, binding reactivated the *in vitro* amino acid polymerizing system to roughly 70% of the wild-type control (Figure 1B). These data are in agreement with the previous report, which showed the yeast stalk assembling to be a coordinated process, in which the P1A protein provides a ribosome an anchor to the P2B protein (*14*).

Characterization of the Oligomeric State of the P1A−P2B Heterocomplex

Size-Exclusion Chromatography. The oligomeric state of the P1A−P2B heterocomplex was investigated using analytical size-exclusion chromatography (SEC). The protein elution profile gave a single, symmetrical peak with a molecular mass of 70 kDa (Figure 2). It should be noted here that the molecular mass measured by SEC is dependent upon the use of globular protein standards. Since the P1A−P2B protein complex was presumed to have an unusual shape (probably with an unstructured C-terminal part, including the hinge region), its shape might differ from that of globular proteins. Thus, the molecular mass was verified by other methods. We used the homo-bifunctional cross-linker, glutaraldehyde (GA). After SEC analysis, the protein complex was cross-linked and analyzed by SDS−PAGE. The analysis showed two major bands with apparent molecular masses of ∼14 and ∼28 kDa, indicating that the dimeric form is present in the solution (Figure 2 inset). It should be stressed here that there are no higher oligomeric forms to be detected via SDS−PAGE after cross-linking.

Dynamic Light Scattering (DLS). To further characterize the behavior of the P1A−P2B complex *in vitro*, we used dynamic light scattering as a supplementary method. The DLS experiment indicated that only one species occurred predominantly in the solution because the polydispersity of the protein solution was low. Indeed, the width of distribution of molecular dimensions of the particles undergoing Brownian motion was estimated to be 25.3% (0.82 nm) of their mean value, and the polydispersity index was calculated to be 0.06. This indicates that mainly one class of complexes was present in solution. The D_T measured at different protein concentrations and extrapolated to a concentration of zero was 664×10^{-9} cm^2/s, and the R_H value was 3.36 nm. The molecular mass was 54 kDa, estimated from the hydrodynamic radius, assuming a globular protein model derived from the R_H value. The results from DLS experiments resembled the data obtained by the SEC approach, but differed from those of the cross-linking experiment. All these data were taken as a strong indication of a nonspherical shape of the molecule and were in agreement with observations by cryoelectron microscopy (*23*). Indeed, molecular masses estimated by DLS or by SEC are reliable only if the molecule is a sphere, that is to say, if one can write $f_{sphere} = 6\pi\eta R = 1.05$, where f is the friction coefficient related to the diffusion one by the usual Stokes−Einstein relationship. The frictional ratio (f_{exp}/f_{sphere}) of the heterocomplex presented here is calculated to be 1.35, which clearly shows that the hetero-complex is a nonspherical molecule.

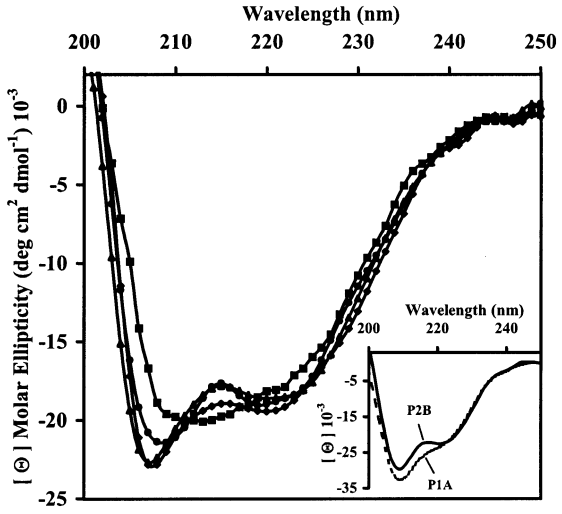

FIGURE 3: Effect of different pH values on far-UV CD data of the P1A−P2B heterocomplex: (▲) pH 7.5, (◆) pH 9.0, (●) pH 5.0, and (■) pH 2.0. The inset shows CD data analysis of separate P1A and P2B proteins.

Structural Characterization

Circular Dichroism Spectroscopy. Analyses of individual proteins P1A and P2B at pH 7 show the proteins to contain significant amounts of α-helical segments (Figure 3 inset), where P2B has a more clear helical pattern than P1A, which has more random coil. The CD data obtained for the separate P proteins are in agreement with earlier studies (*2*, *3*), which imply the existence of isolated secondary structure elements, missing stabilizing tertiary side chain interactions from native separate P proteins. In contrast, the CD spectra of the heterocomplex displayed the typical features for α-helical proteins with two minima at 208 and 222 nm (Figure 3). Virtually all CD spectra from various pH conditions were superimposable, with one exception: the spectrum recorded when the pH was decreased below the pI of the proteins forming the complex. At pH 2, the shape of the spectrum changed, in a way that the two minima characteristic of α-helices disappeared, and the third one became more visible at ∼215 nm, indicating that substantial amounts of *β*-sheets may have been formed. Such spectral transition with a change in pH has been already observed for the individual P1A protein under similar conditions (*3*).

Secondary Structure Calculation. Various empirical methods have been developed for analysis of protein CD spectra toward quantitative estimation of the secondary structure, number, and length of structural elements, and also for assignment of the protein tertiary class. For CD data deconvolution, we used a CDPro software package (*41*, *42*), which contains the following programs: quantitative estimation of the secondary structure content (CONTIN/LL, SELCON3, and CDSSTR) and the protein tertiary class assignment (CLUSTER). It should be noted here that this package utilizes CD spectra of globular proteins with known X-ray structures as a template, as well as data from denatured proteins for a better representation of unordered structures. Our analysis showed that the P1A−P2B heterocomplex could be ranked among the tertiary class of all-α proteins, and the average α-helical content, calculated using the three programs, was ∼65% (Figure 4A), including ∼40% of regular α-helix (α_R) and 25% of distorted α-helix (α_D). The root-mean-square deviation (rmsd) was low, in the range of 0.10−0.25, indicating a good performance of the programs. The number of structural elements was estimated to be six α-helices with an average length of 12 amino acids per α-helix. The analysis of spectra for P1A and P2B showed that these individual proteins have α-helical contents of ∼60%. (Figure 4A inset). The rmsd was also low, and did not exceed 0.25. Our CD experimental data were further compared with data from a theoretical analysis performed with the aid of the EVA Web-based server, evaluating automatic structure prediction servers continuously and objectively. All programs used for the analysis showed a high content of α-helical structure, up to 70%, with five to six α-helices with an average length of 10 amino acids, which is in good agreement with the CD experimental data (Figure 4B). Virtually, two regions could be distinguished in the polypeptides. The first 70 amino acids are formed by four α-helices, with a probability of ∼1, and this region is involved in protein−protein interactions, as previously described (*47*). The second region, containing the flexible hinge and the cluster of charged and hydrophobic amino acids, can also adopt an α-helical structure, with one α-helix for P1A and two for P2B; however, the probability is quite low, in the range of 0.4−0.6. These data suggest that the 70 N-terminal amino acids might have a well-ordered structure, followed by less ordered fragments which could gain its compact structure upon binding to its natural partner(s).

Thermal Denaturation. Thermal denaturation was followed by monitoring changes in dichroic intensities at 222 nm upon heating at various pHs (Figure 5). At neutral pH, the individual P proteins, particularly P1A, showed an absence of cooperative unfolding, indicating that they could have a noncompact structure, the so-called molten globule, as reported previously (*2*, *3*). Interesting data emerged from temperature-induced unfolding of the heterocomplex. At neutral and alkaline pH, the CD signal showed full cooperative transitions and implied a two-state folding−unfolding transition, characteristic of globular proteins with a well-defined hydrophobic core. At pH 5, we observed that the structure of the heterocomplex was more stable until a certain high temperature and then disappeared almost noncooperatively; at this pH, DLS data indicated that the complex was prone to generate polydisperse high-molecular mass oligomeric forms (data not shown), which might make a significant contribution to the stability of the structure. At pH 2, the heterocomplex does not go through any transition, indicating the absence of specific tertiary structure at any temperature, even if a secondary structure is present under these conditions. This behavior of the heterocomplex resembles that found for the isolated P1A protein observed previously (*3*), indicating that the complex is fully denatured under such conditions.

Equilibrium Denaturation by Urea. We used urea-induced unfolding of the P1A−P2B heterocomplex to further characterize the structural stability. The changes in circular dichroism as a function of urea concentration show that the denaturation of the complex is fully cooperative, following closely a two-state transition mechanism (Figure 6), while the P proteins alone lack a two-state folding−unfolding transition (Figure 6, inset A). This indicates that the heterocomplex has a well-packed hydrophobic core, and that the protein complex has gained a stable tertiary structure in

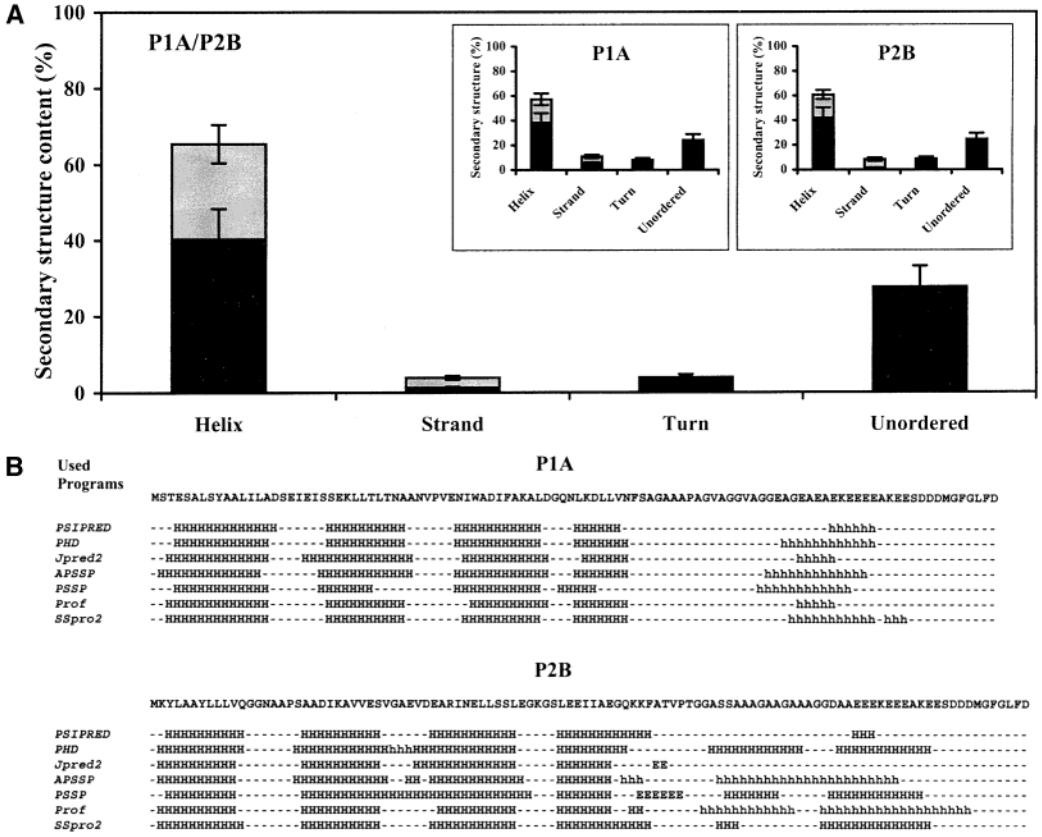

FIGURE 4: Secondary structure analysis. (A) Estimation of protein secondary structure from circular dichroism spectra. Regular and distorted α-helices are marked in black and gray, respectively. Insers represent analysis for separate P proteins. (B) Secondary structure prediction for separate P1A and P2B proteins. Prediction was performed using several programs (see Materials and Methods). Uppercase H's stand for a probability of helical structure close to 1 and lowercase h's for a probability of ∼0.5.

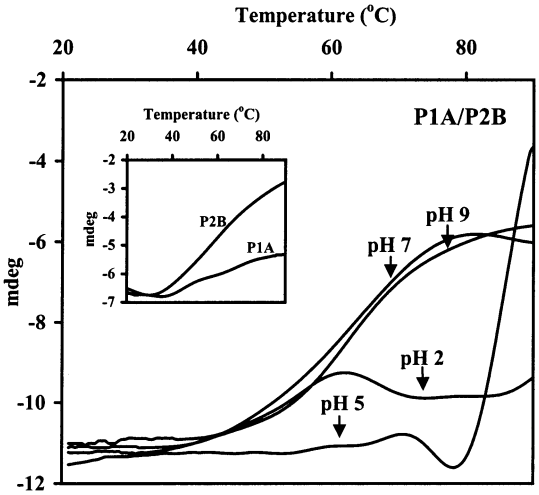

FIGURE 5: Thermal denaturation profile of the P1A−P2B heterocomplex. Ellipticity at 222 nm was monitored as a function of temperature at the indicated pH values. The inset shows the thermal denaturation of separate P1A and P2B proteins at neutral pH.

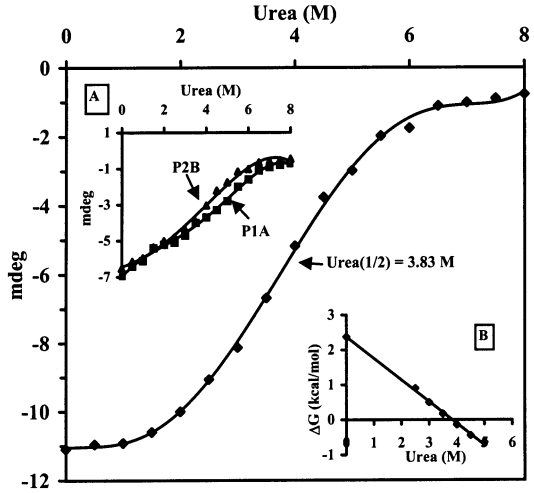

FIGURE 6: Urea denaturation of the heterocomplex. Ellipticity at 222 nm was monitored as a function of urea concentration at pH 7. Inset A shows a plot of millidegrees at 222 nm of separate P1A and P2B proteins vs urea concentration, performed at neutral pH. Inset B represents the ΔG for the heterocomplex as a function of urea concentration, where $\Delta G(H_2O) = 2.37$ kcal/mol and $m = 0.62$ kcal mol^{-1} M^{-1}.

forming the heterocomplex. At pH 7.0, the unfolding of the complex started at ∼2.5 M urea and was essentially completed in 5.5 M urea, with the transition midpoint at 3.8 M urea (Figure 6). Fitting the denaturation curve to a two-state model for the unfolding transition mechanism resulted in thermodynamic parameters calculated for pH 7.0. The free energy difference in the absence of denaturant, ΔG_{H_2O}, was 2.37 kcal/mol. The parameter describing the cooperativity of the transition, m, was found to be 0.62 kcal mol^{-1} M^{-1}.

Intrinsic Fluorescence Properties. In the P1A−P2B heterocomplex, there is only one tryptophan residue located in the native P1A protein at position 41. It makes intrinsic fluorescence an excellent probe for investigating conformational changes in the environment around the fluorophore. Fluorescence was investigated selectively by excitation at two different wavelengths: for tyrosine and tryptophan

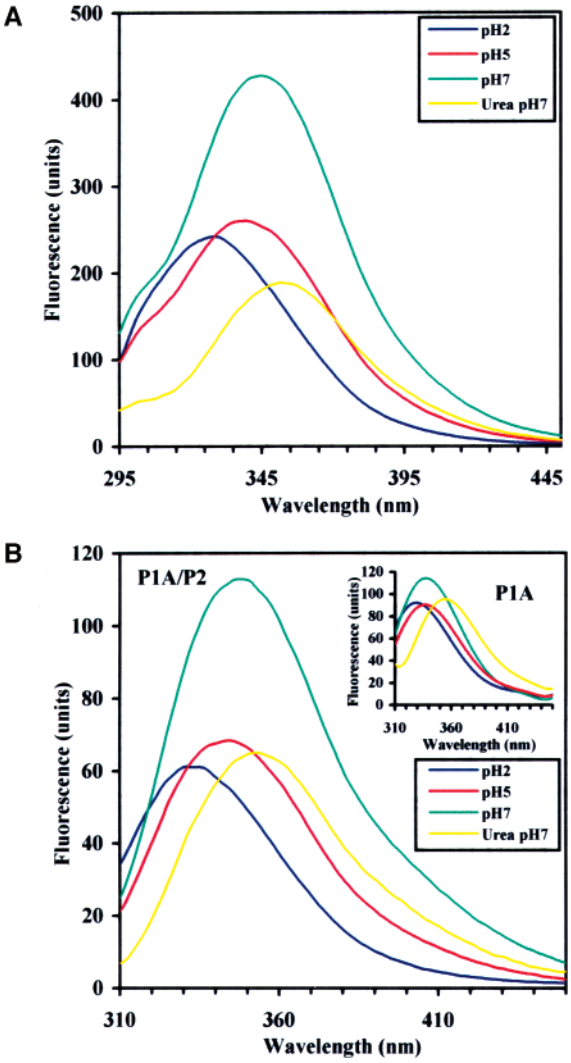

FIGURE 7: Intrinsic fluorescence of the heterocomplex: (A) excitation at 280 nm and (B) excitation at 295 nm. The inset shows fluorescence spectra of the P1A protein alone. Spectroscopic conditions are described in Materials and Methods.

residues at 280 nm and for tryptophan alone at 295 nm. The emission spectra were collected at 295−450 and 310−450 nm, respectively. The fluorescence spectrum for tyrosine and tryptophan residues (excitation at 280 nm) showed a maximum centered at 345 nm (Figure 7A), while excitation at 295 nm for the single tryptophan gave an emission spectrum with a maximum at 348 nm (Figure 7B). In a control experiment, the tryptophan residue in the P1A protein alone exhibited maximum emission centered at 335 nm (Figure 7B inset), which could be attributed to the fact that this residue had been buried in the hydrophobic environment. The alkaline pH had no significant influence on the spectra (data not shown), whereas a shift to acidic conditions had a significant effect on the emission spectra. At pH 5.0, excitation at 280 nm, a blue shift was observed toward 339 nm, and with excitation at 295 nm, the blue-shifted emission maximum was observed at 344 nm and the fluorescence intensity decreased significantly. A pH of 2.0 had an even more pronounced effect: the emission maxima moved to a shorter wavelengths, close to 320 nm, typical of an indole group in a hexane solution. This suggests tryptophan 41 is more buried in the hydrophobic environment, and may explain an aggregation tendency of the complex at acidic

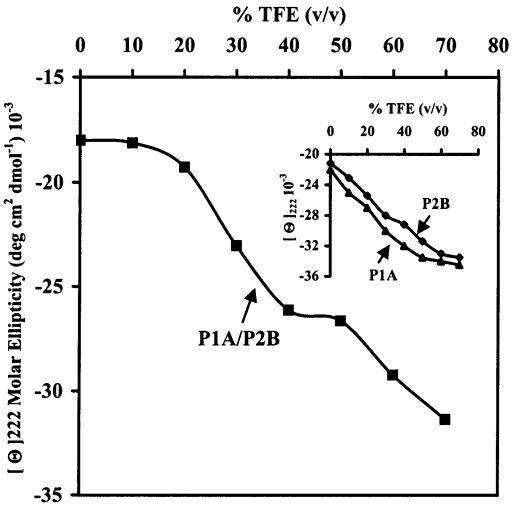

FIGURE 8: Changes in molar residue ellipticities $[\Theta]_{222}$ measured at 222 nm shown as a function TFE concentration. The inset shows a plot of $[\Theta]_{222}$ of a separate P1A and P2B proteins vs TFE percentage (v/v).

pH, as observed by light scattering (data not shown). Interestingly, pH conditions do not exert any significant influence on the emission spectra of tryptophan in the P1A protein (Figure 7B inset), having maxima at 334 nm at pH 5 and 329 nm at pH 2, indicating that the protein has already been in higher-order oligomeric forms, which would support our previous observations by SEC analysis (*10*). Unfolding of the heterocomplex with urea resulted in a strong decrease in the fluorescence emission spectra and a concomitant red shift of the maximum to 353 nm, corresponding to the fluorescence maximum of tryptophan in aqueous solution, implying that under native conditions, the heterocomplex may have well-packed side chains, where tryptophan might make some contribution to the formation of the hydrophobic core. It should be stressed here that the tyrosine emission spectrum is well-marked, occurring as a shoulder with the maximum centered at 303 nm in the native as well as in the denatured state (Figure 7A). Even at acidic pH, the shoulder is well-marked, indicating a large distance between tyrosine residues (located at the C-terminal part of the P1A and P2B proteins) and tryptophan 41, and thereupon, energy transfer does not occur efficiently, implying that both amino acids are located far from each other in the native protein.

Effect of Trifluoroethanol on the Folding Transition. Conformational changes in the heterocomplex were monitored as a function of trifluoroethanol (TFE) concentration and far-UV CD molar ellipticity at 222 nm. Upon addition of TFE, the transition appears to occur in a highly cooperative manner, resembling a two-state transition, yet with some further changes (Figure 8). It should be noted that there are few, if any, pretransition changes in the far-UV CD spectrum of the heterocomplex, when exposed to a low concentration of TFE (0−15%, v/v), the very characteristic of compact polypeptides. On the other hand, the secondary structure of the P1A−P2B complex is appreciably perturbed at a moderately high concentration of TFE (15−40%, v/v). The effectiveness of TFE is thought to level off beyond a concentration of 50%, corresponding to the viscosity maximum of a TFE/water mixture. In the case of the heterocomplex, a CD signal reached a plateau at 40−50% TFE, which could be regarded as a post-transition state; however, a

further increase in far-UV CD molar ellipticity at 222 nm with increasing TFE concentrations beyond the main transition was observed, and thus, the transition is not strictly two-state, as TFE-stabilized states are likely to represent an ensemble of interconverting structures. There is *a priori* no reason the transition should be two-state. Indeed, it is possible that TFE denaturation of proteins may result in states that are neither helical nor native-like, but which are substantially unfolded (*48*). Alternatively, the first transition may be to a state which does not have native compactness but an increased helical structure, and then expands to an open helical state after addition of more cosolvent. The latter has been shown to be the case of denaturation of cytochrome *c* or hen lysozyme by methanol (*49*, *50*). Unlike the heterocomplex, the helical content of separate P1A and P2B proteins after additions of TFE increases continuously (Figure 8 inset) without an appreciable saturation phase.

DISCUSSION

The intent and primary focus of this study was to characterize the biophysical properties of the heterocomplex composed of yeast acidic ribosomal proteins P1A and P2B. Since there is experimental evidence that individual P proteins (P1A and P2B) in solution are in flexible states, which could be regarded as a "molten globule"-like structure (*2*, *3*), the question of when they adopt a stable compact structure arises (upon interaction with each other or during interaction with other ribosomal components). We have shown earlier that P1A and P2B proteins specifically form a hetero-oligomeric complex (*10*). The results of this report allow us to conclude that P1A and P2B proteins display a low level of sequence complexity, as was shown before (*2*, *3*); however, upon binding to each other, they are able to adopt a folded state in the absence of other ribosomal components. The conclusion was drawn on the basis of experiments performed with several biophysical means, such as SEC, cross-linking, DLS, CD, and fluorescence spectroscopy. Such a behavior is rather rare for ribosomal proteins, because the majority of ribosomal proteins cannot form a stable tertiary structure in a solution without additional ribosomal components.

The biological functionality of the P1A−P2B heterocomplex was analyzed to confirm that the complex formed of the recombinant proteins reflects its native biological structure. Thus, the heterocomplex composed of P1A and P2B proteins is able to bind to ribosomes deprived of all P1 and P2 proteins, and moreover can stimulate the activity of ribosomal particles in the *in vitro* polyphenylalanine synthesis assay, yet not to the full extent (Figure 1). Addition of the second pair of P proteins (P1B and P2A) increases the ribosomal polymerizing activity to the full extent (unpublished results). Thus, the obtained data indicate that the complex in question is fully functional and can be used for further structural analysis.

Although there was some biological evidence that the heterocomplex should form a dimer (*12*), physical evidence of such a state has not been fully elucidated in a yeast model. Knowing that the stalk components form an elongated structure on the ribosomal particles (*23*), one may expect that the heterocomplex in a solution could be unusual in size and shape, so we used several techniques for molecular mass determination. SEC analysis gave a molecular mass of ∼70 kDa, quite different from the expected value for a dimer. However, it is well-known that the elution time can vary significantly with the size and shape of proteins. The symmetric shape of the elution profile indicates that the complex occurs as a single species, without any additional oligomeric forms. Further evidence about the molecular mass of the complex was acquired from DLS studies, revealing a molecular mass of 54 kDa. The discrepancy in molecular mass between the two techniques indicates that the shape characteristic of the molecule is unusual. That is to say, the Stokes radius of the molecule is significantly altered and may bring a deviation in elution time, as well as a wrong estimation of the R_H value. The ultimate answer was provided by analysis of the frictional ratio of 1.35, revealing that the complex is a nonspherical, elongated molecule. These data are in agreement with observations made with low-resolution cryo-EM (*23*), where the complex was seen as a protein structure protruding from the 60S ribosomal subunit. Furthermore, the high mobility of the stalk components in prokaryotic as well as in eukaryotic ribosomes has been observed (*51*). It is highly possible that the heterocomplex occurs as a dimer in the solution, as observed in a cross-linking experiment. A substantial amount of the monomeric form was observed in the cross-linking experiment. However, this can be attributed to the fact that quantitative cross-linking is rarely accomplished. Additionally, it should be pointed out that there were no higher-oligomeric forms on the SDS−PAGE. Moreover, the DLS data point out that the protein solution is monodisperse, because the polydispersity index was calculated to be 0.06, thus underscoring the idea that the dimeric form of the heterocomplex is the only possible species to be observed in the solution. What is more, homo-oligomers were not observed in SEC analysis (data not shown), further underscoring the idea of heterodimers.

The secondary structure of the P1A−P2B heterocomplex consists primarily of α-helix as determined by CD spectroscopy, and the protein could be classified among the tertiary class all-α proteins. The experimentally estimated α-helical content of the complex, having 65% α-helix, agrees well with the value obtained from theoretical calculation. Furthermore, our CD analysis of single P proteins has shown an α-helix content of ∼60% polypeptide, closely resembling the theoretical prediction, and is similar to the value represented by the polypeptides in the complex. There are some discrepancies between our secondary structure estimation of individual P proteins and data obtained in previous work (*3*, *4*). Previously, Zurdo et al. reported α-helical contents of 11 and 28% for P1A and P2B proteins, respectively. This inconsistency might arise from different methods of protein purification. Previously, proteins were purified under native conditions, which could result in misfolded proteins, and the α-helical content of the individual proteins reflects a random-coil structure rather than a molten globule-like state. In our case, proteins were purified in the presence of a denaturation agent (*30*), which upon refolding could adopt the appropriate fold given their small size. Our data are consistent with the generally accepted observation that polypeptides in the molten globule state have a native secondary structure, but lack well-packed side chains (*4*).

The results obtained from several different techniques, such as TFE titration and thermal or urea unfolding, indicate

that although single polypeptides display a lack of cooperativity in unfolding as previously suggested (*2*, *3*), the behavior of the heterocomplex can be generally fitted to a two-state model, typical of folded proteins with a well-defined hydrophobic core. Thus, it is possible to conclude that when two polypeptides bind to each other, protein ordering is taking place, and a rigid tertiary structure is formed. On the basis of the accumulated data, one can venture the idea that the first 70 amino acids, where four α-helices were predicted, may adopt a globular structure composed of four-helix bundles. With regard to the tertiary structure of the prokaryotic stalk protein L12, the functional counterpart of the eukaryotic P proteins, structural similarities are rather scarce. First of all, there is no similarity in the primary structure. Second, in the case of L12, the first 35 amino acids form two helices involved in dimer formation (*26*, *28*); on the other hand, the P protein's much bigger N-terminal domain, composed of 70 amino acids, might form a helical structure composed of four-helix bundles, which is involved in dimer formation as well. Another divergence in tertiary structure between both proteins is located in the C-terminus, where L12 has a rigid structure composed of α-helices and β-strands (*25*, *26*), while the P proteins might adopt a helical structure composed of one or two α-helices. Fluorescence data showed that tryptophan and tyrosine residues might bring some stabilization to the overall tertiary structure, but it should be emphasized here that these two types of residues are far away from each other because efficient energy transfer does not take place between them. When only tryptophan is considered, there are significant differences between the heterocomplex and the individual P1A protein. In the P1A−P2B arrangement, this residue is more exposed to the solvent, having the emission spectrum shifted toward the red range, while tryptophan in the P1A protein has its emission spectrum located in the blue wavelength, suggesting thus this protein might be in a higher-oligomeric form where tryptophan could make a significant contribution to this state. For the heterocomplex, such a state is observed only at acidic pH, in which the overall net charge of proteins is significantly reduced, and hydrophobic forces may predominate in the protein environment. These data may indicate that this residue is not fully involved in stabilization of the heterocomplex structure, but it is also possible for tryptophan 41 to be an important point in interaction with the P0 ribosomal protein.

With such evidence as this, it is possible to answer the question raised in the beginning of this section; the analyzed P proteins are able to gain a stable 3D structure upon binding to each other, and are probably present in the cytoplasm as a stable dimer which can directly interact with the 60S ribosomal subunit. Formation of the dimer is likely to take place just after the polypeptides emerge from the active ribosome, and presumably, the dimer is an intrinsic form of these polypeptides. Molten globule-like structure of individual P proteins could be considered in two ways: it might be a kinetic intermediate important for folding, yet on the other hand, it could be an off-pathway nonproductive species that is the energetically preferred form of single P proteins, and that is present only under *in vitro* conditions. This latter idea could be supported by the fact that single P proteins, especially those from the P1 group, are extremely unstable in the cytoplasm when unbound to their partners (*19*), underscoring the idea that the heterodimer is the only natural form of these proteins.

ACKNOWLEDGMENT

We are indebted to Professor Juan P. G. Ballesta (Universidad Autónoma de Madrid, Madrid, Spain) for quadruply disrupted strain D4567 and also for critical reading of the manuscript and valuable remarks.

REFERENCES

1. Wright, P. E., and Dyson, H. J. (1999) Intrinsically unstructured proteins: Re-assessing the protein structure−function paradigm, *J. Mol. Biol. 293*, 321−331.
2. Zurdo, J., Sanz, J. M., Gonzales, C., Rico, M., and Ballesta, J. P. G. (1997) The exchangeable yeast ribosomal acidic protein YP2β shows characteristics of a partly folded state under physiological conditions, *Biochemistry 36*, 9625−9635.
3. Zurdo, J., Gonzalez, C., Sanz, J. M., Rico, M., Remacha, M., and Ballesta, J. P. G. (2000) Structural differences between *Saccharomyces cerevisiae* ribosomal stalk proteins P1 and P2 support their functional diversity, *Biochemistry 39*, 8935−8943.
4. Ptitsyn, O. B. (1995) Molten globule and protein folding, *Adv. Protein Chem. 47*, 83−229.
5. Tchorzewski, M. (2002) The acidic ribosomal P proteins, *Int. J. Biochem. Cell Biol. 34*, 911−915.
6. Wool, I. G., Chan, Y. L., Gluck, A., and Suzuki, K. (1991) The primary structure of rat ribosomal proteins P0, P1 and P2 and a proposal for a uniform nomenclature for mammalian and yeast ribosomal proteins, *Biochimie 73*, 861−870.
7. Bailey-Serres, J., Vangala, S., Szick, K., and Lee, C.-H. K. (1997) Acidic phosphoprotein complex of 60S ribosomal subunit of maize seedling roots, *Plant Physiol. 114*, 1293−1305.
8. Planta, R. J., and Mager, W. H. (1998) The list of cytoplasmic ribosomal proteins of *Saccharomyces cerevisiae*, *Yeast 14*, 471−477.
9. Tchorzewski, M., Boldyreff, B., Issinger, O.-G., and Grankowski, N. (2000) Analysis of the protein−protein interactions between the human acidic ribosomal P-proteins: evaluation by the two hybrid system, *Int. J. Biochem. Cell Biol. 32*, 737−746.
10. Tchorzewski, M., Boguszewska, A., Dukowski, P., and Grankowski, N. (2000) Oligomerization properties of the acidic ribosomal P-proteins from *Saccharomyces cerevisiae*: effect of P1A protein phosphorylation on the formation of the P1A−P2B hetero-complex, *Biochim. Biophys. Acta 1499*, 63−73.
11. Guarinos, E., Remacha, M., and Ballesta J. P. G. (2001) Asymmetric interactions between the acidic P1 and P2 proteins in the *Saccharomyces cerevisiae* ribosomal stalk, *J. Biol. Chem. 276*, 32474−32479.
12. Shimizu, T., Nakagaki, M., Yoshinori, N., Kobayashi, Y., Hachimori, A., and Uchiumi, T. (2002) Interaction among silkworm ribosomal proteins P1, P2 and P0 required for functional protein binding to the GTPase-associated domain of 28S rRNA, *Nucleic Acids Res. 30*, 2620−2627.
13. Gonzalo, P., Lavergne, J. P., and Reboud, J. P. (2001) Pivotal role of the P1 N-terminal domain in the mammalian ribosomal stalk and in the proteosynthesic activity, *J. Biol. Chem. 276*, 19762−19769.
14. Zurdo, J., Parada, P., van den Berg, A., Nusspaumer, G., Jimenez-Diaz, A., Remacha, M., and Ballesta, J. P. G. (2000) Assembly of *Saccharomyces cerevisiae* ribosomal stalk: binding of P1 proteins is required for the interaction of P2 proteins, *Biochemistry 39*, 8929−8934.
15. Ballesta, J. P. G., and Remacha, M. (1996) The large ribosomal subunit stalk as a regulatory element of the eukaryotic translational machinery, *Prog. Nucleic Acid Res. Mol. Biol. 55*, 157−193.
16. Ballesta, J. P. G., Rodriguez-Gabriel, M. A., Bou, G., Briones, E., Zambrano, R., and Remacha, M. (1999) Phosphorylation of the yeast ribosomal stalk. Functional effects and enzymes involved in the process, *FEMS Microbiol. Rev. 23*, 537−550.
17. Vard, C., Guillot, D., Bargis, P., Lavergne, J.-P., and Reboud, J. P. A. (1997) A specific role for the phosphorylation of mammalian acidic ribosomal protein P2, *J. Biol. Chem. 272*, 20259−20262.

18. Zambrano, R., Briones, E., Remacha, M., and Ballesta, J. P. G. (1997) Phosphorylation of the acidic ribosomal P proteins in *Saccharomyces cerevisiae*: a reappraisal, *Biochemistry 36*, 14439−14446.
19. Nusspaumer, G., Remacha, M., and Ballesta, J. P. G. (2000) Phosphorylation and N-terminal region of yeast ribosomal protein P1 mediate its degradation, which is prevented by proteins P2, *EMBO J. 19*, 6075−6084.
20. Remacha, M., Jimenez-Diaz, A., Bermejo, B., Rodriguez-Gabriel, M. A., Guarions, E., and Ballesta, J. P. G. (1995) Ribosomal acidic phosphoproteins P1 and P2 are not required for cell viability but regulate the pattern of protein expression in *Saccharomyces cerevisiae*, *Mol. Cell. Biol. 15*, 4754−4762.
21. Tchorzewski, M., Boldyreff, B., and Grankowski, N. (1999) Extraribosomal function of acidic ribosomal P1-protein YP1α from *Saccharomyces cerevisiae*, *Acta Biochim. Pol. 46*, 901−910.
22. Ito, T., Chiba, T., Ozawa, R., Yoshida, M., Hattori, M., and Sakaki, Y. (2001) A comprehensive two-hybrid analysis to explore the yeast protein interactome, *Proc. Natl. Acad. Sci. U.S.A. 98*, 4569−4574.
23. Gomez-Lorenzo, M. G., Spahn, C. M., Agrawal, R. K., Grassucci, R. A., Penczek, P., Chakraburtty, K., Ballesta, J. P., Lavandera, J. L., Garcia-Bustos, J. F., and Frank, J. (2000) Three-dimensional cryo-electron microscopy localization of EF2 in the *Saccharomyces cerevisiae* 80S ribosome at 17.5 Å resolution, *EMBO J. 19*, 2710−2718.
24. Liljas, A., and Gudkov, A. T. (1987) The structure and dynamics of ribosomal protein L12, *Biochimie 69*, 1043−1047.
25. Leijonmarck, M., Eriksson, S., and Liljas, A. (1980) Crystal structure of a ribosomal component at 2.6 Å resolution, *Nature 286*, 824−826.
26. Wahl, M. C., Bourenkov, G. P., Bartunik, H. D., and Huber, R. (2000) Flexibility, conformational diversity and two dimerization modes in complexes of ribosomal protein L12, *EMBO J. 19*, 174−186.
27. Bocharov, E. V., Gudkov, A. T., and Arseniev, A. S. (1996) Topology of the secondary structure elements of ribosomal protein L7/L12 from *E. coli* in solution, *FEBS Lett. 379*, 291−294.
28. Chandra Sanyal, S., and Liljas, A. (2000) The end of the beginning: structural studies of ribosomal proteins, *Curr. Opin. Struct. Biol. 10*, 633−636.
29. Shimmin, L. C., Ramirez, G., Matheson, A. T., and Dennis, P. P. (1989) Sequence alignment and evolutionary comparison of the L10 equivalent and L12 equivalent ribosomal proteins from archaebacteria, eubacteria and eukaryotes, *J. Mol. Evol. 29*, 448−462.
30. Tchorzewski, M., Boguszewska, A., Abramczyk, D., and Grankowski, N. (1999) Overexpression in *Escherichia coli*, purification, and characterization of recombinant 60S ribosomal acidic proteins from *Saccharomyces cerevisiae*, *Protein Expression Purif. 15*, 40−47.
31. Szyszka, R., Boguszewska, A., Grankowski, N., and Ballesta, J. P. G. (1995) Differential phosphorylation of ribosomal acidic proteins from yeast cell by two endogenous protein kinase: casein kinase-2 and 60S kinase, *Acta Biochim. Pol. 42*, 357−362.
32. Pace, C. N. (1986) Determination and analysis of urea guanidine hydrochloride denaturation curves, *Methods Enzymol. 131*, 267−280.
33. Pace, C. N., Shirley, B. A., and Thomson, J. A. (1989) Measuring the conformational stability of a protein, in *Protein structure: a practical approach* (Rickwood, D., and Hames, B. D., Eds.) pp 311−330, Oxford University Press, Oxford, U.K.
34. Eyrich, V. A., Marti-Renom, M. A., Przybylski, D., Madhusudhan, M. S., Fiser, A., Pazos, F., Valencia, A., Sali, A., and Rost, B. (2001) EVA: continuous automatic evaluation of protein structure prediction servers, *Bioinformatics 12*, 1242−1243.
35. Jones, D. (1999) Protein secondary structure prediction based on position-specific scoring matrices, *J. Mol. Biol. 292*, 195−202.
36. Rost, B. (1996) PHD: predicting one-dimensional protein structure by profile based neural networks, *Methods Enzymol. 266*, 525−539.
37. Cuff, J. A., and Barton, G. J. (1999) Evaluation and improvement of multiple sequence methods for protein secondary structure prediction, *Proteins 34*, 508−519.
38. Raghava, G. P. S. http://imtech.ernet.in/raghava/apssp (2002).
39. Rost, B. http://cubic.bioc.columbia.edu/predictprotein (2002).
40. Pollastri, G., Baldi, P., Fariselli, P., and Casadio, R. (2001) Improved prediction of the number of residue contacts in proteins by recurrent neural networks, *Bioinformatics 17*, S234−S242.
41. Sreerama, N., and Woody, R. W. (2000) Estimation of protein secondary structure from circular dichroism spectra: comparison of CONTIN, SELCON, and CDSSTR methods with an expanded reference set, *Anal. Biochem. 287*, 252−260.
42. Sreerama, N., Venyaminov, S. Y., and Woody, R. W. (2000) Estimation of protein secondary structure from circular dichroism spectra: inclusion of denatured proteins with native proteins in the analysis, *Anal. Biochem. 287*, 243−251.
43. Andrade, M. A., Chacon, P., Merelo, J. J., and Moran, F. (1993) Evaluation of secondary structure of proteins from UV circular dichroism spectra using an unsupervised learning neural network, *Protein Eng. 6*, 383−390.
44. Gill, S. C., and von Hippel, P. H. (1989) Calculation of protein extinction coefficients from amino acid sequence data, *Anal. Biochem. 182*, 319−326.
45. Laemmli, U. K. (1970) Cleavage of structural proteins during assembly of the head of bacteriophage T4, *Nature 277*, 680−685.
46. Boguszewska, A., Tchórzewski, M., Dukowski, P., Winiarczyk, S., and Grankowski, G. (2002) Subcellular distribution of the acidic ribosomal P-proteins from *Saccharomyces cerevisiae* in various environmental conditions, *Biol. Cell 94*, 139−146.
47. Jose, M. P., Santana-Roman, H., Remacha, M., Ballesta, J. P., and Zinker, S. (1995) Eukaryotic acidic phosphoproteins interact with the ribosome through their amino-terminal domain, *Biochemistry 34*, 7941−7948.
48. Arakawa, T., and Goddette, D. (1985) The mechanism of helical transition of proteins by organic solvents, *Arch. Biochem. Biophys. 240*, 21−32.
49. Kamatari, Y. O., Konno, T., Kataoka, M., and Akasaka, K. (1996) The methanol-induced globular and expanded denatured states of cytochrome *c*: a study by CD fluorescence, NMR and small-angle X-ray scattering, *J. Mol. Biol. 259*, 512−523.
50. Kamatari, Y. O., Konno, T., Kataoka, M., and Akasaka, K. (1998) The methanol-induced transition and the expanded helical conformation in hen lysozyme, *Protein Sci. 7*, 681−688.
51. Cowgill, C. A., Nichols, B. G., Kenny, J. W., Butler, P., Bradbury, E. M., and Traut, R. R. (1984) Mobile domains in ribosomes revealed by proton nuclear magnetic resonance, *J. Biol. Chem. 259*, 15257−15263.

BI0206006